Published in final edited form as:
J Control Release. 2010 April 2; 143(1): 71–79. doi:10.1016/j.jconrel.2009.12.022.

Endocytic uptake of a large array of HPMA copolymers: Elucidation into the dependence on the physicochemical characteristics

Jihua Liu[a], **Hillevi Bauer**[a], **Jon Callahan**[b], **Pavla Kopečková**[a,b], **Huaizhong Pan**[a], and **Jindřich Kopeček**[a,b,*]

[a] Department of Pharmaceutics and Pharmaceutical Chemistry/CCCD, University of Utah, Salt Lake City, UT 84112, USA

[b] Department of Bioengineering, University of Utah, Salt Lake City, UT 84112, USA

Abstract

Endocytic uptake and subcellular trafficking of a large array of HPMA (*N*-(2-hydroxypropyl) methacrylamide) based copolymers possessing positively or negatively charged residues, or hydrophobic groups were evaluated by flow cytometry and living cell confocal microscopy in cultured prostate cancer cells. The degrees of cellular uptake of various copolymer fractions with narrow polydispersities were quantified. The copolymer charge was the predominant physicochemical feature in terms of cellular uptake. Fast and efficient uptake occurred in positively charged copolymers due to non-specific adsorptive endocytosis, whereas slow uptake of negatively charged copolymers was observed. The uptake of copolymers was also molecular weight dependent. The copolymers were internalized into the cells through multiple endocytic pathways: positively charged copolymers robustly engaged clathrin-mediated endocytosis, macropinocytosis and dynamin-dependent endocytosis, while weakly negatively charged copolymers weakly employed these pathways; strongly negatively charged copolymers only mobilized macropinocytosis. HPMA copolymer possessing 4 mol% of moderately hydrophobic functional groups did not show preferential uptake. All copolymers ultimately localized in late endosomes/lysosomes via early endosomes; with varying kinetics among the copolymers. This study indicates that cell entry and subsequent intracellular trafficking of polymeric drug carriers are strongly dependent on the physicochemical characteristics of the nanocarrier, such as charge and molecular weight.

Keywords

HPMA copolymer; endocytic uptake; physicochemical characteristics; charge; intracellular traffickings

*Corresponding author: Jindřich Kopeček, Center for Controlled Chemical Delivery, 20 S 2030 E, BPRB 205B, University of Utah, Salt Lake City, UT 84112-9452, USA. Phone: (801) 581-7211; Fax: (801) 581-7848. jindrich.kopecek@utah.edu (J. Kopeček).

1. Introduction

Employment of macromolecular drug carriers for the delivery of anticancer therapeutics has resulted in significant improvements in treatment efficacy [1]. A variety of macromolecular drug carriers are currently under investigation. An ideal macromolecular drug carrier should possess preferable pharmacokinetics, highly efficient cellular uptake and preferential subcelluar trafficking. These biological merits are determined to a large extent by physicochemical characteristics of the macromolecular drug carriers. For instance, molecular weight has an impact on the intravascular half-life and renal clearance [2]. Positively charged macromolecular drug carriers are internalized by cells more efficiently than negatively charged carriers, however their uptake occurs in the majority of cells [3]. Nevertheless, how the physicochemical characteristics of drug carriers determine their uptake and subcellular trafficking remains largely unknown.

Understanding the uptake and subcellular trafficking of macromolecular drug carriers by cells relies on knowledge of the complexity and diversity of endocytic pathways. Many endocytic pathways have been identified and a variety of classification schemes have been proposed. Based on the cargo, endocytosis is classified as phagocytosis or pinocytosis (fluid-phase endocytosis) [4]. Based on receptors, endocytosis can be designated as receptor mediated endocytosis specified by involvement of specific high-affinity receptors, adsorptive endocytosis denoted by nonspecific binding of solutes to the cell membrane, and regular endocytosis taking up surrounding fluid unspecifically [5]. Most common classification schemes of endocytosis are based on protein machinery that facilitates the process, such as clathrin-mediated endocytosis, and clathrin independent endocytosis [5–8]. Clathrin independent endocytosis is further categorized as caveolae-mediated endocytosis and clathrin- and caveolin-independent endocytosis [5,7] or dynamin dependent and dynamin independent endocytosis [7,8]. Dynamin is a GTPase protein that surrounds the neck of vesicle pits and facilitates the scission of many, but not all vesicles, such as clathrin-coated, caveolae-mediated and clathrin- and caveolin-independent vesicles [9]. Macropinocytosis is a distinct pathway of pinocytosis [5,10,11]; traditionally, macropinocytosis was designated as bulk non-selective and constitutive uptake of extracellular fluid through plasma membrane protrusion or ruffling. It has been recently recognized as an elaborately coordinated process including actin-mediated membrane reorganization and regulation of signaling, such as phosphoinositide (PI) 3-kinases [10,11].

Hydrophilic and neutral copolymers of *N*-(2-hydroxypropyl)methacrylamide (HPMA) have been broadly used as linear water soluble polymeric drug carriers for therapeutic applications [12,13]. Several drug-polymer conjugates based on HPMA copolymers have been studied clinically. A doxorubicin-HPMA copolymer conjugate PK1 was the first HPMA copolymer drug conjugate to enter clinical trials [14]. Phase II trial of PK1 in breast, non-small cell lung and colorectal cancers suggested that polymer-bound therapeutics are capable of improving anticancer a ctivities [15]. PK2 [16], a compound related to PK1, and several HPMA copolymer drug conjugates containing taxol, camptothecin, and platinum entered Phase I clinical trials [17–20]. HPMA copolymers are internalized into cells through endocytosis as shown in an early study on HPMA copolymers containing different degradable peptidyl side chains using rat visceral yolk sacs cultured in vitro [21]. Incorporation of hydrophobic tyrosinamide residues, bound either directly to the polymer main chain or through a glycylglycine linker, enhanced the uptake of HPMA copolymers [22]. More recently, endocytic uptake and subcellular trafficking of a HPMA antibody conjugate have been studied [23].

In the present study, the relationship between the mechanisms of endocytic uptake and subcellular trafficking of a large array of fluorescently-labeled, HPMA based copolymers and their physicochemical characteristics, such as charge, molecular weight and hydrophobicity,

was studied. The array was composed of 9 HPMA copolymers with 5 comonomers possessing functional groups with positive or negative charges or containing a short hydrophobic peptide. FITC-labeled polyHPMA (P-FITC) was used as control. These copolymers were fractionated using size exclusion chromatography to create parallel Mw "ladders" consisting of 10 narrowly polydisperse fractions with molecular weights ranging from 10 to 200 kDa. Cellular uptake of the HPMA copolymer fractions and involvement of different endocytic pathways were assessed by flow cytometry in cultured prostate cancer cells. Subcellular trafficking of membrane vesicles carrying copolymers was characterized by living cell confocal microscopy.

2. Materials and methods

Materials

All chemicals and solvents used were of reagent grade or better unless otherwise stated. The monomers, MAA (methacrylic acid), SEMA (2-sulfoethyl methacrylate), DEMA (2-(*N*,*N*-dimethylamino)ethyl methacrylate), and MATC (methacryloyloxyethyl trimethylammonium chloride) were purchased from PolySciences (Warrington, PA), Alexa Fluor 647-labeled dextran 10 kDa and Hoechst 33342 were purchased from Molecular Probes (Carlsbad, CA). Chlorpromazine, filipin complex, mevinolin, Dynasore, 5-(*N*-ethyl-*N*-isopropyl)-amiloride, LY 294002, and wortmannin were from Sigma-Aldrich (St. Louis, MO). Lipofectamine 2000 was from Invitrogen (Carlsbad, CA). The plasmids encoding RFP-Rab5 and RFP-Rab7 were purchased from Addgene (Cambridge, MA).

2.1 Polymer synthesis, fractionation and characterization—The HPMA copolymers were prepared as described in [24]. The general copolymerization scheme, structures of comonomers used, and example of molecular weight profiles are shown in Scheme 1. The composition of copolymers is shown in Table 1. For the sake of clarity, the polymers were named based on the content of comonomers in the feed for the initial polymer array. All polymers were further fractionated by SEC (size exclusion chromatography) using a Superose 6 HR 16/60 column. Parallel molecular weight "ladders" consisting of 10 narrowly polydisperse fractions with molecular weights ranging from 10 to 200 kDa were created.

The molecular weight of the final polymer fractions was determined using a Superose 6 HR10/30 column (AKTA/FPLC) in PBS, equipped with UV, RI and laser light scattering detector (MiniDAWN). The ASTRA software from Wyatt Technology, (Santa Barbara) was used for the calculation of molecular weights.

The content of FITC in copolymers was determined by UV-Vis spectrometry (Varian Cary 400 Bio UV-Visible Spectrophotometer) using the absorbance at 495 nm ($\varepsilon_{495\ nm}$ = 80000 M^{-1} cm^{-1}) in 0.1 M borate buffer (pH 9). The content of peptide (GFLG) groups in the copolymer was determined by HPLC amino acid analysis [24]. The content of charged groups (MAA, SEMA, and DEMA) in the copolymers was measured using an automated TIM854 pH titration workstation (Titralab, Radiometer Analytical, Lyon, France) with a combined minitype electrode. Solution of 0.05 N NaOH or 0.05 N HCl was used as titration standards. Content of MATC was measured by potentiometric titration of chloride ions using a combined silver type electrode and 0.05 M $AgNO_3$ titration standard solution.

2.2 Zeta potential measurement—The zeta potentials were measured using Zetasizer Nano ZS according to manufacturer's instruction as described in Supplementary Data.

2.3 Cell line—C4-2, a gift from Dr. Ursula Elsässer-Beile, was a subline of LNCaP that was one of the most commonly used prostate cancer cell line [25,26]. C4-2 cells were maintained in RPMI 1640 medium supplemented with 10% fetal bovine serum (FBS) at 37 °C in an incubator with 5% CO_2. All experiments were performed in the presence of 10% FBS.

2.4 Confocal laser scanning microscopy—HPMA copolymers containing different functional groups (0.2 mg/ml) were incubated with cells in medium containing 10% FBS at 37 °C for the indicated time periods. After incubation, live-cell fluorescence imaging was performed immediately using Olympus confocal microscope (FV 1000). The detailed method is described in Supplementary Data.

2.5 Quantitative study of uptake by flow cytometry—The cells were seeded in 12-well plates at a density of 2.5×10^5 cells per well and incubated in medium for 1 day (37 °C, 5% CO_2). Then cells were incubated with copolymers at 37 °C for the indicated time periods. The concentration of copolymers used was 0.1 mg/ml in this type of study. After incubation, medium was removed. Cells were harvested and washed with PBS three times followed immediately by flow cytometry analysis. The amount of 1.0×10^4 cells was collected, and the mean fluorescence intensity was recorded for each sample.

2.6 Determination of the amount of copolymers taken up by cells—Mean fluorescence intensity of each sample was converted into amount of copolymer taken up by the cells using flow cytometry and fluorescence plate reader. The fluorescence intensity of copolymers in cells was obtained from both flow cytometry analysis and fluorescence plate reader measurement. Meanwhile, the amount of FITC (ng) in the same sample was measured using the fluorescence plate reader. Hence, based on the content of FITC in each copolymer, the amount of copolymer in cells was derived. The detailed method is described in Supplementary Data.

2.7 Inhibition of uptake via endocytic pathways by selective inhibitors—Cells were pre-incubated in medium containing a selective chemical inhibitor of endocytic pathways for 30 min. Next, polymers were added in the presence of the inhibitor. Then cells were further incubated for certain periods of time and harvested for flow cytometry as described in 2.5. The inhibitors used, their concentrations, and pathways they inhibit are shown in Table S2.

2.8 Cholesterol depletion and disruption—Filipin and mevinolin were used for cholesterol disruption as described in Supplementary Data.

2.9 Transfection—Transfection was performed using Lipofectamine 2000 according to manufacturer's instruction as described in Supplementary Data.

3. Results

3.1. Design and characterization of HPMA copolymers containing different functional groups

A large array of HPMA copolymers with widely disparate functional groups was generated to provide HPMA copolymers with a variety of physicochemical characteristics [24]. For hydrophilic copolymers, four different charged comonomers in two contents were employed to bestow different charge and density on the copolymers: MATC - a strong base, DEMA - a weak base, MAA - a weak acid, and SEMA - a strong acid (Scheme 1). A peptide-containing monomer, *N*-methacryloylglycylphenylalanyl-leucylglycine (MA-GFLG) was utilized to introduce hydrophobicity into the copolymer. Copolymers were named based on the content of comonomers in the feed for the initial polymer array. The content of the copolymers is shown in Table 1. All copolymers were fractionated into 10 molecular weight fractions each with a narrow polydispersity. The fractions designated as "F1" to "F10" by fractionation order exhibited decreasing molecular weight. Molecular weights and characteristics of some of fractions are listed (Table 2 and Table S1).

Cytotoxicity of P-MATC was evaluated in a wide range of concentrations in C4-2 cells after 24 h of incubation. No cytotoxicity occurred in cells exposed to lower concentrations (< 0.4 mg/ml). A slight decrease in cell viability was observed with higher concentrations of P-MATC (> 0.4 mg/ml) (Fig. S1). In the present study, the concentration of copolymer used was not higher than 0.2 mg/ml.

3.2. Types of endocytosis of HPMA copolymers containing different charged groups

Fluid phase endocytosis is observed when membrane vesicles entrapping fluid containing macromolecules transport to late endosomes or lysosomes that accumulate in perinuclear areas. Adsorptive endocytosis occurs when surrounding solutes associate with plasma membrane. In our studies, internalization of copolymers by cells was observed and captured under confocal microscope. For neutral polyHPMA (P-FITC) and copolymers possessing weakly negatively charged groups (P-MAA20), no internalization was detectable within 30 min incubation (Fig. 1a. A and E). The visible perinuclear localization of these copolymers was noticed after incubation for 4 h (Fig. 1a. B and F) and was more significant after prolonged incubation (Fig. 1a. C and G). For copolymers possessing strongly negatively charged groups (P-SEMA20), perinuclear localization of copolymers only appeared after 12 h of incubation with cells (Fig. 1a. K). Unlike neutral or negatively charged copolymers, the copolymers possessing strongly positively charged groups (P-MATC20) were seen to quickly (within 10 min) associate with the whole plasma membrane after exposure to cells (Fig. 1a. Q), displaying characteristic adsorptive endocytosis. Subsequently, the membrane-associated pattern gradually disappeared and was replaced by an intracellular pattern, indicating that these membrane-associated copolymers were endocytosed into cells (Fig. 1a. S). The copolymers possessing weakly positively charged groups (P-DEMA20) behaved similarly but less dramatically (Fig. 1a. M-O). In addition, P-FITC and HPMA copolymers containing different functional groups were found to co-localize with dextran 10 kDa, a fluid phase endocytosis marker (Fig. 1a. D, H, L, P and T). Hence, HPMA copolymers containing different charged groups were internalized into cells through different types of endocytosis. The neutral homopolymer and negatively charged copolymers were internalized into cells via fluid phase endocytosis, whereas positively charged copolymers by adsorptive endocytosis.

3.3. The rate of uptake of HPMA copolymers containing comonomer units of different charge

Flow cytometry was used to quantify the endocytic uptake of copolymers possessing charged groups (Fig. 1b). Mean fluorescence intensity of each sample was obtained and converted into amount of copolymer taken up by the cells (see 2.6 and Supplementary Data). Positively charged copolymers, P-MATC20 and P-DEMA20, were taken up much more efficiently than polyHPMA (P-FITC) or copolymers containing negatively charged groups, P-MAA20 and P-SEMA20. The uptake of copolymers containing negatively charged groups, P-MAA20 and P-SEMA20, decreased when compared to P-FITC. Maximum uptake occurred with the strongly positively charged copolymer, P-MATC20, whereas least uptake took place with the strongly negatively charged copolymer, P-SEMA20; P-MATC5 and P-DEMA5 did not show significant increase in uptake, and P-SEMA5 and P-MAA5 did not show significant decrease of uptake compared to polyHPMA (P-FITC), probably due to a low content of charged groups. Thus, the rate of uptake of HPMA copolymers was determined by the structure and content of the charged groups.

3.4. Kinetics of uptake of HPMA copolymer containing comonomer units of different charge

Based on the significant difference in the rate of uptake between positively and negatively charged HPMA copolymers after incubation for 12 h, a detailed kinetic study of their uptake in C4-2 cells was performed. P-DEMA20 and P-MAA20 were chosen to represent the positively and negatively charged copolymers, respectively. Time points and dosage response

of cells internalizing copolymers were measured. The profile of uptake vs. concentration showed that uptake elevated with increasing concentrations for both copolymers (Fig. 2a). However, the uptake increased in P-DEMA20 more than in P-MAA20 at the same concentration. The higher the concentrations, the more significant differences between P-DEMA20 and P-MAA20 were observed. The profile of uptake vs. time showed the same pattern as that of uptake vs. concentration (Fig. 2b). The prolonged incubation enhanced uptake for both copolymers. The uptake of P-DEMA20 and P-MAA20 was both a time- and concentration-dependent process and a higher efficiency of uptake occurred in P-DEMA20, a positively charged copolymer.

3.5. Molecular weight dependent uptake of HPMA copolymers containing charged groups

The effect of molecular weight on the uptake of copolymers was evaluated by flow cytometry analysis. Copolymer fractions were incubated with cells and the uptake was measured. For polyHPMA (P-FITC fractions) and negatively charged copolymers (P-MAA20 fractions), it was shown that the lower the molecular weight, the higher the uptake (Fig. 3). In contrast, the uptake of positively charged copolymers (P-DEMA20 fractions) decreased with decreasing molecular weight. These results suggest that uptake of HPMA copolymer containing charged groups is molecular weight dependent, but that the charge still has a greater impact on endocytosis.

3.6. Endocytic pathways of HPMA copolymers containing different charged groups

Selective inhibitors were utilized to examine the endocytic pathways through which HPMA copolymers containing different charges were internalized into C4-2 cells. In order to compare the inhibited uptake of neutral, and positively and negatively charged copolymers, a 12 h interval of incubation was chosen because the strongly negatively charged copolymers needed 12 h to be internalized to a level, at which the fluorescent intensity was high enough to be reproducibly quantified. To prevent the possibility that prolonged incubation time might generate cytotoxicity, the inhibitor concentrations chosen were considerably lower than that used by other authors [27–31] (Table S2). We found that at concentration used the inhibitors did not create cytotoxicity after 12 h incubation.

Decreased uptake was observed for all copolymers in cells treated with chlorpromazine (CPZ), a selective inhibitor of clathrin-mediated endocytosis (Fig. 4a). Uptake of all copolymers was not inhibited by filipin and mevinolin, two cholesterol disrupting agents, and caveolae-mediated endocytosis inhibitors (Fig. 4b). Therefore, it appeared that caveolin-mediated endocytosis was not employed in the internalization of HPMA copolymers containing charged groups. This is due to the lack of caveolin-1 expression, a major protein component of the caveolar pits in C4-2 cells [32]. Dynasore, a chemical inhibitor of dynamin, has been recently utilized to determine the involvement of dynamin in the endocytic pathways [33]. Uptake of positively charged copolymers (P-DEMA5; P-DEMA20; P-MATC5; P-MATC20) was dramatically diminished whereas uptake of negatively charged copolymers (P-MAA5; P-MAA20; P-SEMA5; P-SEMA20) was only slightly reduced (Fig. 3c). The involvement of macropinocytosis was investigated by using commonly used pathway inhibitors, such as amiloride, a Na/K ion exchanger blocker, and wortmannin and LY 294002, two PI3 kinase inhibitors. The amounts of uptake inhibition by these three inhibitors were comparable for the same copolymer. Uptake was suppressed by three inhibitors for both positively and negatively charged copolymers. Uptake of positively charged copolymers (P-DEMA5; P-DEMA20; P-MATC5; P-MATC20) was suppressed considerably more than that of negatively charged copolymers (P-MAA5; P-MAA20; P-SEMA5; P-SEMA20) (Fig. 4d).

The contribution of each pathway to endocytosis varied in response to structures of copolymers containing different charged groups. Clathrin-mediated endocytosis, dynamin dependent

pathway and macropinocytosis are utilized by copolymers with a higher content of negatively charged groups (P-SEMA20 and P-MAA20). However, more significantly decreased uptake was seen in copolymers containing weak acid groups (P-MAA20) than in strong negatively charged copolymers (P-SEMA20) by inhibition of all three pathways, indicating that relatively low contribution of each pathways results in overall low uptake. Uptake of P-SEMA20 was shown to decrease more remarkably by blocking macropinocytosis, suggesting that copolymers containing strong acid groups are predominantly internalized through this pathway. Uptake of positively charged copolymers (P-DEMA20 and P-MATC20) was inhibited severely by inhibitors of clathrin-mediated, dynamin-dependent endocytosis and macropinocytosis, indicating all these pathways vigorously participated in the internalization of positively charged copolymers. However, more significant inhibition of P-MATC20 uptake occurred when exposed to inhibition of clathrin-mediated endocytosis. In contrast, diminished uptake after inhibition of dynamin dependent endocytosis and macropinocytosis appeared more significant in P-DEMA20 than in P-MATC20. This demonstrated that charge and strength of charge have an impact on the mobilization of endocytic pathways. In addition, uptake of copolymers containing a lower content of charged comonomers (P-MATC5, P-DEMA5, P-SEMA5 and P-MAA5) was inhibited in all three pathways, to an extent similar to P-FITC, indicating that the low content of acid or basic comonomers did not result in alteration of physicochemical characteristics significant enough for regulation of endocytic pathways.

3.7. Uptake of HPMA copolymer possessing hydrophobic groups

The uptake of P-GFLG, a HPMA copolymer containing short hydrophobic tetrapeptide side-chains was compared with copolymers containing hydrophilic charged groups as described above. It was similar to P-FITC and copolymers with low content of charged groups (P-SEMA5, P-MAA5, P-DEMA5 and P-MATC5), indicating that the hydrophobic group when present at low concentration (4 mol%) does not play a dominant role in terms of cellular uptake (Fig. S2). Moreover, the relationship between uptake of P-GFLG and molecular weight was assessed. It showed that the uptake of P-GFLG occurred in a molecular weight dependent manner similar to P-FITC (Fig. S3).

3.8. Intracellular trafficking of HPMA copolymers with charged groups

To explore the intracellular trafficking of HPMA copolymers with different charged groups, we chose to visualize the two important stations on the endocytic routes: early endosomes and late endosomes. Rabs, small GTPases, are localized at distinct membrane vesicles and responsible for membrane vesicle formation, development and trafficking [34,35]. To visualize early and late endosomes, C4-2 cells were overexpressed with RFP fused Rab5, an early endosome membrane associated protein, and Rab7, a late endosome membrane associated protein. Within 10 min after exposure to P-DEMA20, vesicles entrapping P-DEMA20 already fused with early endosomes (Fig. 5). The copolymers resided in early endosomes for more than one hour and then started appearing in late endosomes. On the contrary, P-MAA20 appeared in visualized endosomes in 45 min and late endosomes in 4 h after incubation, much slower than P-DEMA20. These findings coincide with the above data on slow cell entry of negatively charged copolymers.

4. Discussion

Understanding of the interdependent roles that fundamental physicochemical characteristics of drug carriers play on the cellular uptake and intracellular trafficking is extremely important. For instance, one can design polymeric drug carriers with physicochemical characteristics that enable polymer-drug conjugates to be taken up efficiently or to enrich the proper membrane confined organelles, such as endosomes or lysosomes. Therefore, suitable endosomal escape

or lysosomal enzymatic cleavage can be chosen to warrant efficient release of drugs from their carriers.

The fact that positive charge is a major physicochemical characteristic in a variety of drug carriers promoting uptake has been realized for more than two decades [3,36]. The positive charge contributes to higher efficiency of uptake by interaction with cell membrane in polyethylenimine (PEI) [37]. Nanoparticles based on D,L-polylactide (PLA) and poly(ethylene glycol-co-lactide) containing cationic lipid stearylamine demonstrated a preferential uptake compared to that without lipid stearylamine, reported by Altschuler and coworkers [38]. The amine-terminated polyamidoamine (PAMAM) dendrimers possess a higher rate of cellular uptake than carboxyl-terminated or hydroxyl-terminated dendrimers [39].

The impact of incorporated charged groups on cellular uptake of HPMA copolymers was assessed in our study. The highly efficient cellular uptake of copolymers possessing positive charge was confirmed, in agreement with studies from other groups. Furthermore, we observed the rapid association of positively charged copolymers (P-DEMA20 and P-MATC20) with plasma membrane and subsequent localization in late endosomes, indicating that positively charged copolymers are indeed internalized via adsorptive endocytosis. Due to the attractive electrostatic force between negatively charged plasma membrane and positively charged cations, the presence of cationic residues on the surface of a hydrophilic and uncharged macromolecule leads to non-specific adsorptive pinocytosis [40,41]. Recently, phosphatidylserine, the abundant anionic phospholipid in the bilayer, was recognized to participate in the electrostatic interactions of positively charged macromolecules with negatively charged membranes [42]. Adsorptive endocytosis can be highly efficient and lead to uptake rates two or three orders of magnitude greater than rates found with cargo macromolecules captured only in the fluid phase [40,41]. This might confer cationic macromolecules as reasonable drug carriers. However, some of their intrinsic properties restrict their application, such as toxicity associated with nonspecific binding to all cells if positive charged groups are not masked. To overcome this, targeted cationic drug carriers need to be developed by incorporation of targeting moieties to target to specific cells.

Molecular weight is an important feature that affects cellular uptake. However, our data indicated that the charge was dominant over molecular weight in the effect on cellular uptake. Nevertheless, uptake of positively and negatively charged copolymers correlated distinctively with molecular weight. The positively charged copolymers with higher molecular weight contain more positively charged groups and generate a stronger attractive electrostatic force, leading to elevated uptake. On the contrary, the negatively charged copolymers with higher molecular weight have more negatively charged groups and produce a stronger repulsive electrostatic force, resulting in diminished uptake. This correlates with a study of nanoparticles based on chitosan, a polycationic polymer, which showed a superior uptake of higher molecular weight nanoparticles than that of low molecular weight particles, in correlation with the ζ potential [43].

The charge also influences the endocytic pathways of HPMA copolymers in C4-2 cells. Various studies have been undertaken to investigate the mechanisms of cellular uptake and intracellular trafficking of macromolecular drug carriers with different charged groups. Studies revealed that three specific endocytic pathways - the clathrin-mediated endocytosis, the caveolae-mediated endocytosis and macropinocytosis facilitate internalization of PEI-DNA polyplexes in some cells [44]. DeSimone and coworkers studied the internalization of microfabricated monodisperse cylindrical particles in a variety of cells. Positively charged particles were internalized mainly through clathrin-mediated endocytosis and macropinocytosis [45]. Kannan et al. demonstrated that G3.5-COOH anionic PAMAM dendrimers appeared to be primarily internalized by caveolae-mediated endocytosis in A549 lung epithelial cells while cationic G4-

NH_2 and neutral G4-OH dendrimers appeared to be taken in by a non-clathrin, non-caveolae mediated mechanism [39].

Our data showed that multiple pathways including clathrin-mediated endocytosis, dynamin dependent endocytosis and macropinocytosis are involved in the internalization of HPMA copolymers containing different charged groups. However, these pathways are not actively involved in the uptake of weakly negatively charged copolymers (P-MAA20) due to repulsive electrostatic forces and consequently, less effective activation of endocytosis compared to positively charged copolymers. Even more dramatically, strongly negatively charged copolymers (P-SEMA20) appeared to be internalized only through macropinocytosis. It is in concert with an extremely low uptake due to strong repulsive electrostatic force as determined in the quantification study.

For positively charged copolymers (P-DEMA20 and P-MATC20), clathrin-mediated endocytosis, dynamin-dependent endocytosis and macropinocytosis vigorously participated in their internalization. A more significant inhibition of uptake occurred in strongly positively charged copolymers (P-MATC20) via clathrin-mediated endocytosis when compared to weakly positively charged copolymers (P-DEMA20). Moreover, less significant inhibition of uptake of strongly positively charged copolymers (P-MATC20) appeared through dynamin-dependent and macropinocytosis, compared to weakly positively charged copolymers (P-DEMA20). These data demonstrate that clathrin-mediated endocytosis is a major pathway by which strongly positively charged copolymers are internalized by C4-2 cells.

In addition, for positively charged copolymers (P-DEMA20 and P-MATC20), inhibition of clathrin-mediated endocytosis showed less remarkable effect than that of dynamin-dependent endocytosis and macropinocytosis, likely because of compensation of uptake by activation of clathrin-independent pathways [38]. Schmid and coworkers observed compensation for the loss of clathrin-mediated endocytosis by alternative clathrin-independent endocytosis [46]. They listed several reasons to explain this phenomenon. First, distinct endocytic vesicles target to distinct intracellular destinations. Second, distinct pathways could be differentially regulated. Third, alternate pathways may serve the rebalancing of plasma membrane metabolism [47]. Exactly how these compensatory responses are regulated remains to be elucidated.

It is worth mentioning that we only demonstrated the trend of relative contribution of each pathway to endocytosis in the present study due to the method of utilizing selective inhibitors. No inhibitor is able to inhibit an endocytic pathway to 100%, which makes the contribution that each pathway contributes to total endocytic activity difficult to achieve. Moreover, there have been no other approaches generally applicable for quantitative determination of the contribution of each endocytic mechanism. Exploration in this field relies on further insight into the mechanism and function of these endocytic pathways.

Incorporation of hydrophobic groups into HPMA copolymers did not give rise to adsorptive endocytosis; an enhanced uptake compared to hydrophilic, neutral polyHPMA was not observed. It is important to note that the content of hydrophobic groups in P-GFLG was only 4 mol%. In a previous study on HPMA copolymers containing tyrosinamide residues, an enhanced rate of endocytosis was observed at substitutions above 10 mol% [22]. Therefore, low concentration of hydrophobic residues might be a major reason for unenhanced cellular uptake. In addition, we speculated that the formation of unimolecular micelles with hydrophobic groups buried inside and hydrophilic polymer main chains outside may be another contributing factor. This is supported by early studies on solution properties of HPMA copolymers containing p-nitroaniline (drug model) or meso-chlorin e_6 monoethylenediamine (photosensitizer) using light scattering and other approaches [48–50].

Understanding a macromolecule's intracellular itinerary is important for the rational design of strategies for intracellular drug release. The complexity of membrane vesicle formation and regulation and endocytic routes require advanced techniques to better understand the broader picture. Many studies have visualized endosomes and lysosomes using immunostaining to recognize endosome and lysosome' surface markers in fixed cells. Late endosomes/lysosomes are also often visualized using lysotracker that easily causes diffused pattern [51]. However, these approaches could hinder accurate and correct interpretation of experimental results. To overcome these problems, different approaches have been developed to circumvent fixation artifacts. Duncan et al performed both live cell imaging to delineate the endocytic pathway by means of exogenous addition of physiological markers and post-fixation immune-labeling to define the specific intracellular compartments. Good correlation between two methods enables the confirmation of localization of water-soluble polymeric carriers to specific endocytic compartments [52]. We visualized early and late endosomes via Rab proteins. Unsurprisingly, positively charged copolymer arrived to early and late endosomes more rapidly than negatively charged copolymers.

5. Conclusions

Endocytic uptake of HPMA copolymers is determined by their physicochemical characteristics, such as charge and molecular weight. Positively charged copolymers were internalized into cells through adsorptive endocytosis whereas negatively charged copolymers through fluid phase endocytosis. Fast uptake was observed for positively charged copolymers whereas slow and minimal uptake for negatively charged copolymers. The uptake of copolymers was in a molecular weight dependent manner. In negatively charged copolymers, smaller molecular weights of the copolymers showed greater uptake than higher molecular weight. In contrast, the uptake of positively charged copolymers was enhanced with rising molecular weight. This indicated that a carrier's charge is the predominant physico-chemical feature in terms of cellular uptake. The copolymers entered the cells through multiple endocytic pathways, such as clathrin-mediated endocytosis, dynamin dependent endocytosis and macropinocytosis. Charge and strength of charge play roles in engagement of endocytic pathways. Table 3 shows the relationship between structure and mechanism of cell entry of HPMA copolymers. Strongly charged copolymers demonstrate alterations due to their extreme physico-chemical characteristics; for instance, strongly negatively charged copolymers only can be internalized through macropinocytosis. HPMA copolymer containing 4 mol% of moderately hydrophobic groups was not superior to polyHPMA in terms of cellular uptake possibly due to the low concentration of hydrophobic groups. All copolymers ultimately localized in late endosomes/lysosomes via early endosomes with distinct kinetics, based on the expression of Rab5 and Rab7. This study strongly supports the notion that cellular uptake and intracellular trafficking of polymeric drug carriers are strongly dependent on their physicchemical characteristics, in particular, charge and molecular weight.

Supplementary Material

Refer to Web version on PubMed Central for supplementary material.

Acknowledgments

The research was supported in part by NIH grant CA132831 from the National Cancer Institute. C4-2 prostate cancer cells were kindly provided by Dr. Ursula Elsässer-Beile, University of Freiburg, Germany. We thank Michael Jacobsen for carefully editing the manuscript.

Abbreviations

CPZ	chlorpromazine
DEMA	2-(*N*,*N*-dimethylamino)ethyl methacrylate
FBS	fetal bovine serum
FITC	fluorescein isothiocyanate
GFLG	glycylphenylalanylleucylglycine
HPMA	*N*-(2-hydroxypropyl)methacrylamide
MA	methacryloyl
MAA	methacrylic acid
MATC	*N*-methacryloyloxyethyl trimethylammonium chloride
Mw	weight average molecular weight
Mn	number average molecular weight
P	HPMA copolymer backbone (e.g. P-MAA5 refers to the copolymer of HPMA with MAA with 5% of MAA in the polymerization feed)
PAMAM	polyamidoamine
PEI	polyethylenimine
P-FITC	fluorescein isothiocyanate labeled polyHPMA
RFP	red fluorescent protein
SEMA	2-sulfoethyl methacrylate

References

1. Haag R, Kratz F. Polymer therapeutics: concepts and applications. Angew Chem Int Ed 2006;45(8): 1198–1215.
2. Shiah JG, Dvořák M, Kopečková P, Sun Y, Peterson CM, Kopeček J. Biodistribution and antitumor efficacy of long circulating *N*-(2-hydroxypropyl)methacrylamide copolymer doxorubicin conjugates in nude mice. Eur J Cancer 2001;37:131–139. [PubMed: 11165140]
3. McCormick LA, Seymour LCW, Duncan R, Kopeček J. Interaction of a cationic *N*-(2-hydroxypropyl) methacrylamide copolymer with rat visceral yolk sac cultured in vitro and rat liver in vivo. J Bioact Compatible Polym 1986;1:901–905.
4. Mukherjee S, Ghosh RN, Maxfield FR. Endocytosis. Physiol Rev 1997;77(3):759–803. [PubMed: 9234965]
5. Conner SD, Schmid SL. Regulated portals of entry into the cell. Nature 2003;422(6927):37–44. [PubMed: 12621426]
6. Kirkham M, Parton RG. Clathrin-independent endocytosis: new insights into caveolae and non-caveolar lipid raft carriers. Biochim Biophys Acta 2005;1746(3):349–363. [PubMed: 16440447]
7. Mayor S, Pagano RE. Pathways of clathrin-independent endocytosis. Nat Rev Mol Cell Biol 2007;8 (8):603–612. [PubMed: 17609668]
8. Gong Q, Huntsman C, Ma D. Clathrin-independent internalization and recycling. J Cell Mol Med 2008;12(1):126–144. [PubMed: 18039352]
9. Praefcke GJ, McMahon HT. The dynamin superfamily: universal membrane tubulation and fission molecules? Nat Rev Mol Cell Biol 2004;5(2):133–147. [PubMed: 15040446]
10. Jones AT. Macropinocytosis: searching for an endocytic identity and role in the uptake of cell penetrating peptides. J Cell Mol Med 2007;11(4):670–684. [PubMed: 17760832]
11. Kerr MC, Teasdale RD. Defining macropinocytosis. Traffic 2009;10:364–371. [PubMed: 19192253]

12. Kopeček J. Soluble biomedical polymers. Polim Med 1977;7:191–221. [PubMed: 593972]
13. Kopeček J, Kopečková P, Minko T, Lu ZR. HPMA copolymer – anticancer drug conjugates: Design, Activity, and Mechanism of Action. Eur J Pharmaceutics Biopharm 2000;50:61–81.
14. Vasey PA, Kaye SB, Morrison R, Twelves C, Wilson P, Duncan R, Thomson AH, Murray LS, Hilditch TE, Murray T, Burtles S, Fraier D, Frigerio E, Cassidy J. Phase I clinical and pharmacokinetic study of PK1 [*N*-(2-hydroxypropyl)methacrylamide copolymer doxorubicin]: first member of a new class of chemotherapeutic agents-drug-polymer conjugates, Cancer Res. Campaign Phase I/II Committee. Clin Cancer Res 1999;5(1):83–94. [PubMed: 9918206]
15. Seymour LW, Ferry DR, Kerr DJ, Rea D, Whitlock M, Poyner R, Bolvin C, Hesslewood S, Twelves C, Blackie R, Schätzlein A, Jodrell D, Bissett D, Calvert H, Lind M, Robbins A, Burtles S, Duncan R, Cassidy J. Phase II studies of polymer-doxorubicin (PK1, FCE28068) in the treatment of breast, lung and colorectal cancer. Int J Oncol 2009;34(6):1629–1636. [PubMed: 19424581]
16. Seymour LW, Ferry DR, Anderson D, Hesslewood S, Julyan PJ, Poyner R, Doran J, Young AM, Burtles S, Kerr DJ. Hepatic drug targeting: phase I evaluation of polymer-bound doxorubicin. J Clin Oncol 2002;20(6):1668–1676. [PubMed: 11896118]
17. Meerum Terwogt JM, ten Bokkel Huinink WW, Schellens JH, Schot M, Mandjes IA, Zurlo MG, Rocchetti M, Rosing H, Koopman FJ, Beijnen JH. Phase I clinical and pharmacokinetic study of PNU166945, a novel water-soluble polymer-conjugated prodrug of paclitaxel. Anticancer Drugs 2001;12(4):315–323. [PubMed: 11335787]
18. Schoemaker NE, van Kesteren C, Rosing H, Jansen S, Swart M, Lieverst J, Fraier D, Breda M, Pellizzoni C, Spinelli R, Grazia Porro M, Beijnen JH, Schellens JH, ten Bokkel Huinink WW. A phase I and pharmacokinetic study of MAG-CPT, a water-soluble polymer conjugate of camptothecin. Br J Cancer 2002;87(6):608–614. [PubMed: 12237769]
19. Rice JR, Gerberich JL, Nowotnik DP, Howell SB. Preclinical efficacy and pharmacokinetics of AP5346, a novel diaminocyclohexane-platinum tumor-targeting drug delivery system. Clin Cancer Res 2006;12:2248–2254. [PubMed: 16609041]
20. Rademaker-Lakhai JM, van den Bongard D, Pluim D, Beijnen JH, Schellens JH. A Phase I and pharmacological study with imidazolium-trans-DMSO-imidazole-tetrachlororuthenate, a novel ruthenium anticancer agent. Clin Cancer Res 2004;10(11):3717–3727. [PubMed: 15173078]
21. Duncan R, Rejmanová P, Kopeček J, Lloyd JB. Pinocytic uptake and intracellular degradation of *N*-(2-hydroxypropyl)methacrylamide copolymers. A potential drug delivery system. Biochim Biophys Acta 1981;678(1):143–150. [PubMed: 7306576]
22. Duncan R, Cable HC, Rejmanová P, Kopeček J, Lloyd JB. Tyrosinamide residues enhance pinocytic capture of *N*-(2-hydroxypropyl)methacrylamide copolymers. Biochim Biophys Acta 1984;799(1): 1–8. [PubMed: 6722178]
23. Liu J, Kopečková P, Bühler P, Wolf P, Pan H, Bauer H, Elsässer-Beile U, Kopeček J. Biorecognition and subcellular trafficking of HPMA copolymer – anti-PMSA antibody conjugates by prostate cancer cells. Mol Pharmaceutics 2009;6(3):959–970.
24. Callahan J, Kopečková P, Kopeček J. The intracellular trafficking and subcellular distribution of a large array of HPMA copolymers. Biomacromolecules 2009;10:1704–1714.
25. Horoszewicz JS, Leong SS, Chu TM, Wajsman ZL, Friedman M, Papsidero L, Kim U, Chai LS, Kakati S, Arya SK, Sandberg AA. The LNCaP cell line--a new model for studies on human prostatic carcinoma. Prog Clin Biol Res 1980;37:115–132. [PubMed: 7384082]
26. Wu HC, Hsieh JT, Gleave ME, Brown NM, Pathak S, Chung LW. Derivation of androgen-independent human LNCaP prostatic cancer cell sublines: role of bone stromal cells. Int J Cancer 1994;57(3):406–412. [PubMed: 8169003]
27. Rejman J, Oberle V, Zuhorn IS, Hoekstra D. Size-dependent internalization of particles via the pathways of clathrin- and caveolae-mediated endocytosis. Biochem J 2004;377(Pt 1):159–169. [PubMed: 14505488]
28. Hartung A, Bitton-Worms K, Rechtman MM, Wenzel V, Boergermann JH, Hassel S, Henis YI, Knaus P. Different routes of bone morphogenic protein (BMP) receptor endocytosis influence BMP signaling. Mol Cell Biol 2006;26(20):7791–7805. [PubMed: 16923969]

29. Tsai CC, Lin CL, Wang TL, Chou AC, Chou MY, Lee CH, Peng IW, Liao JH, Chen YT, Pan CY. Dynasore inhibits rapid endocytosis in bovine chromaffin cells. Am J Physiol Cell Physiol 2009;297 (2):C397–406. [PubMed: 19515902]
30. Tagawa M, Yumoto R, Oda K, Nagai J, Takano M. Low-affinity transport of FITC-albumin in alveolar type II epithelial cell line RLE-6TN. Drug Metab Pharmacokinet 2008;23(5):318–327. [PubMed: 18974609]
31. Seastone DJ, Lee E, Bush J, Knecht D, Cardelli J. Overexpression of a novel rho family GTPase, RacC, induces unusual actin-based structures and positively affects phagocytosis in Dictyostelium discoideum. Mol Biol Cell 1998;9(10):2891–2904. [PubMed: 9763450]
32. Bartz R, Zhou J, Hsieh JT, Ying Y, Li W, Liu P. Caveolin-1 secreting LNCaP cells induce tumor growth of caveolin-1 negative LNCaP cells in vivo. Int J Cancer 2008;122:520–525. [PubMed: 17943731]
33. Macia E, Ehrlich M, Massol R, Boucrot E, Brunner C, Kirchhausen T. Dynasore, a cell-permeable inhibitor of dynamin. Dev Cell 2006;10:839–850. [PubMed: 16740485]
34. Rink J, Ghigo E, Kalaidzidis Y, Zerial M. Rab conversion as a mechanism of progression from early to late endosomes. Cell 2005;122(5):735–749. [PubMed: 16143105]
35. Pfeffer S, Aivazian D. Targeting Rab GTPases to distinct membrane compartments. Nat Rev Mol Cell Biol 2004;5(11):886–896. [PubMed: 15520808]
36. Wu GY, Wu CH. Receptor-mediated in vitro gene transformation by a soluble DNA carrier system. J Biol Chem 1987;262:4429–4432. [PubMed: 3558345]
37. Vicennati P, Giuliano A, Ortaggi G, Masotti A. Polyethylenimine in medicinal chemistry. Curr Med Chem 2008;15(27):2826–2839. [PubMed: 18991638]
38. Harush-Frenkel O, Debotton N, Benita S, Altschuler Y. Targeting of nanoparticles to the clathrin-mediated endocytic pathway. Biochem Biophys Res Commun 2007;353(1):26–32. [PubMed: 17184736]
39. Perumal OP, Inapagolla R, Kannan S, Kannan RM. The effect of surface functionality on cellular trafficking of dendrimers. Biomaterials 2008;29(24–25):3469–3476. [PubMed: 18501424]
40. Lloyd JB, Williams KE. Non-specific adsorptive pinocytosis. Biochem Soc Trans 1984;12(3):527–528. [PubMed: 6734911]
41. Lloyd JB, Pratten MK, Duncan R, Kooistra T, Cartlidge SA. Substrate selection and processing in endocytosis. Biochem Soc Trans 1984;12:977. [PubMed: 6530046]
42. Yeung T, Gilbert GE, Shi J, Silvius J, Kapus A, Grinstein S. Membrane phosphatidylserine regulates surface charge and protein localization. Science 2008;319(5860):210–213. [PubMed: 18187657]
43. Huang M, Khor E, Lim LY. Uptake and cytotoxicity of chitosan molecules and nanoparticles: effects of molecular weight and degree of deacetylation. Pharmaceutical Res 2004;21(2):344–353.
44. Mennesson E, Erbacher P, Piller V, Kieda C, Midoux P, Pichon C. Transfection efficiency and uptake process of polyplexes in human lung endothelial cells: a comparative study in non-polarized and polarized cells. J Gene Med 2005;7(6):729–738. [PubMed: 15759254]
45. Gratton SE, Napier ME, Ropp PA, Tian S, DeSimone JM. Microfabricated particles for engineered drug therapies: elucidation into the mechanisms of cellular internalization of PRINT particles. Pharmaceutical Res 2008;25(12):2845–2852.
46. Damke H, Baba T, van der Bliek AM, Schmid SL. Clathrin-independent pinocytosis is induced in cells overexpressing a temperature-sensitive mutant of dynamin. J Cell Biol 1995;131:69–80. [PubMed: 7559787]
47. Lamaze C, Schmid SL. The emergence of clathrin-independent pinocytic pathways. Curr Opin Cell Biol 1995;7(4):573–580. [PubMed: 7495578]
48. Shiah JG, Koňák Č, Spikes JD, Kopeček J. Solution and photoproperties of *N*-(2-hydroxypropyl) methacrylamide copolymer meso-chlorin e_6 conjugates. J Phys Chem B 1997;101(35):6803–6809.
49. Ulbrich K, Koňák Č, Tuzar Z, Kopeček J. Solution properties of drug carriers based on poly[*N*-(2-hydroxypropyl)methacrylamide] containing biodegradable bonds. Makromol Chem 1987;188:1261–1272.
50. Ding H, Kopečková P, Kopeček J. Self-association properties of HPMA copolymers containing an amphipatic heptapeptide. J Drug Targeting 2007;15:465–474.

51. Lemieux B, Percival MD, Falgueyret J. Quantitation of the lysosomotropic character of cationic amphiphilic drugs using the fluorescent basic amine Red DND-99. Anal Biochem 2004;327(2):247–251. [PubMed: 15051542]

52. Richardson SC, Wallom KL, Ferguson EL, Deacon SP, Davies MW, Powell AJ, Piper RC, Duncan R. The use of fluorescence microscopy to define polymer localization to the late endocytic compartments in cells that are targets for drug delivery. J Controlled Release 2008;127(1):1–11.

Appendix A. Supplementary Data

Supplementary data associated with this article can be found, in the online version, at doi: xxx

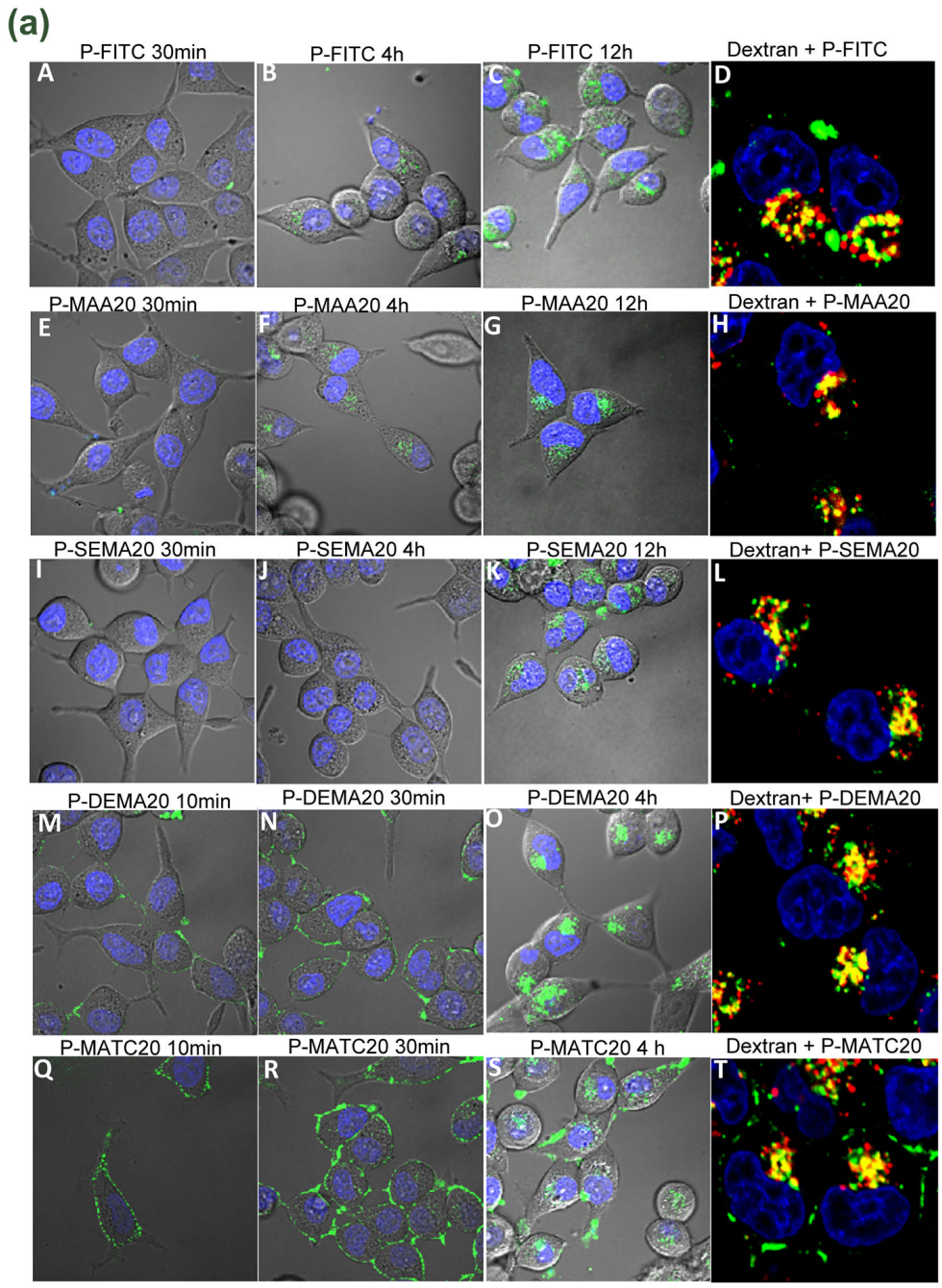

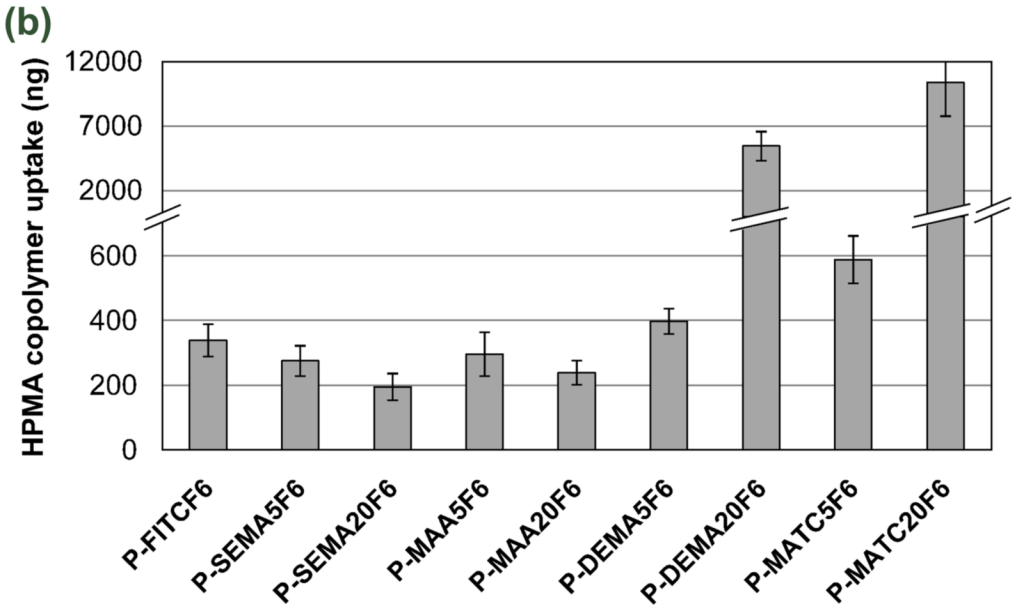

Fig. 1.

Endocytosis and quantification of uptake of HPMA copolymers. C4-2 cells were incubated with fraction 6 (F6) of indicated copolymers. **a)** Endocytosis of copolymers: P-FITCF6 (A-D), P-MAA20F6 (E-H), P-SEMA20F6 (I-L), P-DEMA20F6 (M-P), and P-MATC20F6 (Q-T). Colocalization of copolymers containing different functional groups with dextran 10 kDa, (D, H, L, P and T). C4-2 cells were pre-incubated with fluorescently-labeled dextran 10 kDa for 12 h followed by incubation with copolymer in the absence of dextran. Ten minutes before imaging, Hoechst 33342 was added to visualize nuclei. The green signal indicates FITC labeled copolymers; the red signal indicates dextran; the yellow signal indicates colocalization. All images shown are from one confocal Z slice; they are representative of three separate experiments. **b)** Quantification of uptake of copolymers by flow cytometry. Cells were incubated with F6 of copolymers for 12 h. The data shown are averages (±SD) of four separate experiments. For molecular weights of F6 fractions see Table 2.

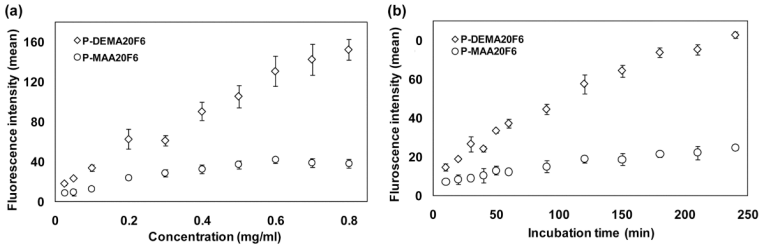

Fig. 2.

Kinetics of uptake of HPMA copolymers with different functional groups. Cells were incubated with copolymers followed by flow cytometry analysis. **a)** Uptake after 4 h in response to different dosages of P-DEMA20F3 and P-MAA20F6. **b)** Time dependent uptake of P-DEMA20F3 (0.1mg/ml) and P-MAA20F6 (0.1mg/ml). The data shown are averages (± SD) of three separate experiments. For molecular weight of fractions see Table 2. Note: Some SDs are too small to be recognized.

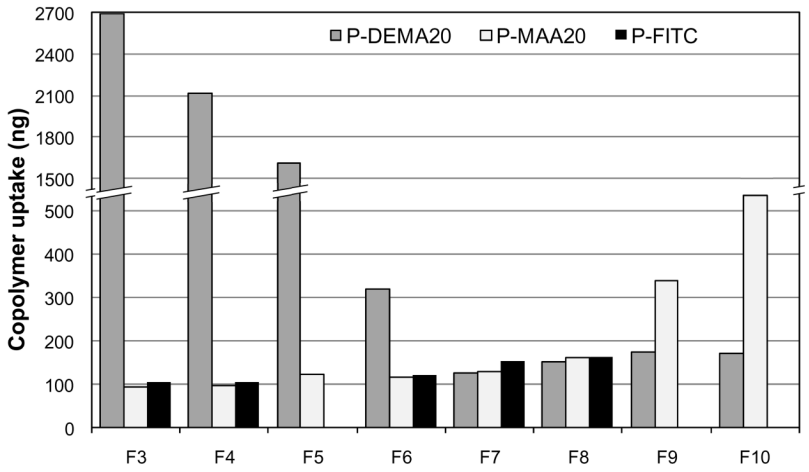

Fig. 3.

Molecular weight dependence of uptake of HPMA copolymers. Cells were incubated with medium containing 0.1 mg/ml of different fractions of P-FITC, P-DEMA20 or P-MAA20 for 12 h. After incubation, cells were harvested for flow cytometry analysis. The data shown are averages (±SD) of three separate experiments. For molecular weight of fractions see Table 3.

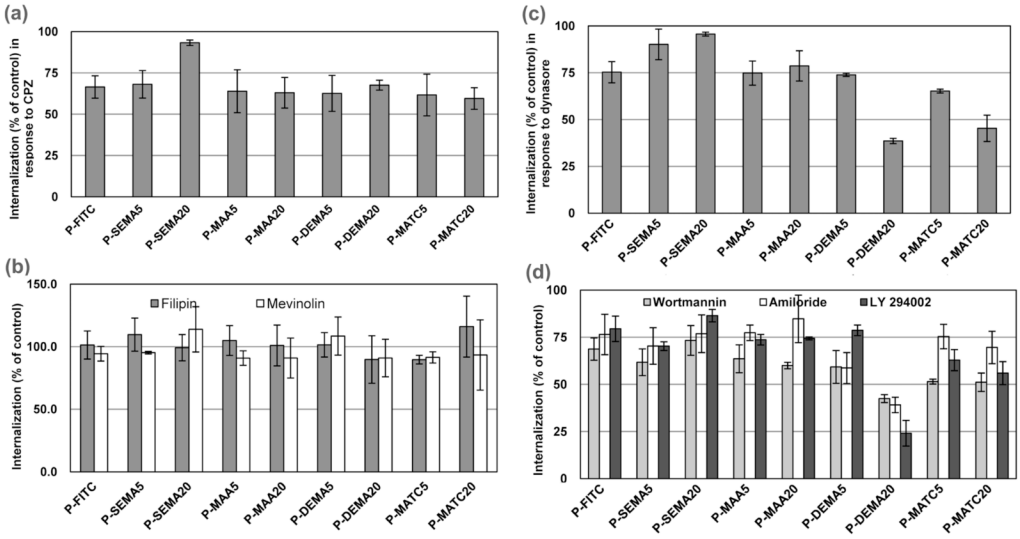

Fig. 4.

Endocytic pathways of HPMA copolymers containing different functional groups. Cells were pre-incubated with inhibitors for 30 min and 0.2 mg/ml fraction 3 (F3) of copolymers were added and incubation continued for 12 h in the presence of inhibitors. After incubation, cells were analyzed by flow cytometry. The data shown are averages (±SD) of three separate experiments. **a)** Clathrin-mediated endocytosis. Cells were exposed to CPZ (10 μM). **b)** Caveolae-mediated endocytosis. Cells were depleted of cholesterol by incubating with serum free medium for 30 min. Subsequently, cells were treated with filipin (2.5 μg/ml; full columns) or mevinolin (10 μM; empty columns) for 30 min prior to exposure to copolymers. **c)** Dynamin-dependent endocytosis. Cells were pre-incubated with dynasore (80 μM). **d)** Macropinocytosis. Cells were pre-treated with wortmannin (1 μM; grey columns), amiloride (10 μM; empty columns), or LY 294002 (10 μM; black columns). For molecular weight of F3 fractions see Table 2.

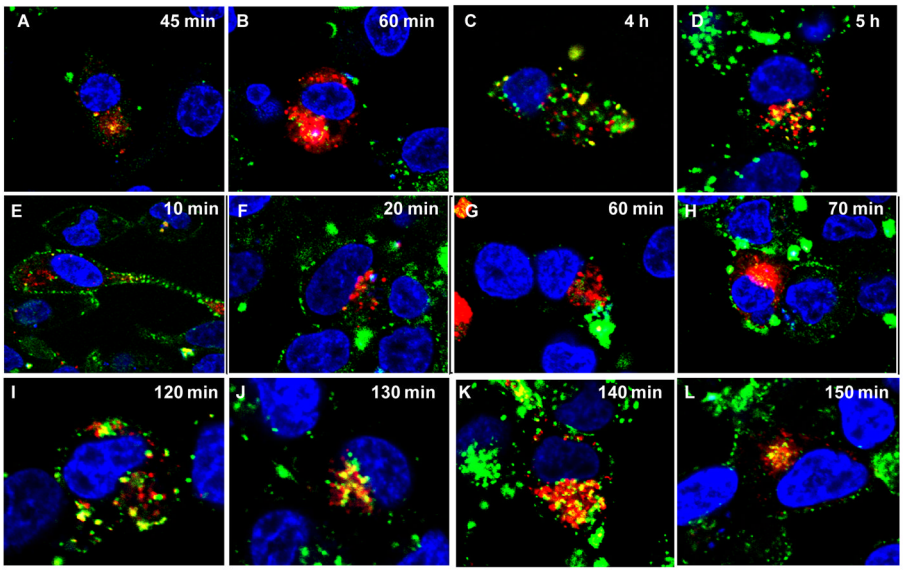

Fig. 5.

Intracellular trafficking of copolymers with different functional groups. C 4-2 cells were transfected with constructs of RFP labeled Rab5 and Rab7. After 24 h, cells were incubated with copolymers, P-DEMA20F4 or P-MAA20F4 for indicated periods of time followed by live cell confocal microcopy. Red signal represents either Rab5 overexpressed early endosomes or Rab7 overexpressed late endosomes, while the green signal signifies membrane vesicles entrapping copolymers. **AB**: Rab5 + P-MAA20; **C-D**: Rab7 + P-MAA20; **E-H**: Rab5 + P-DMA20, and **I-L**: Rab7 + P-DEMA20.

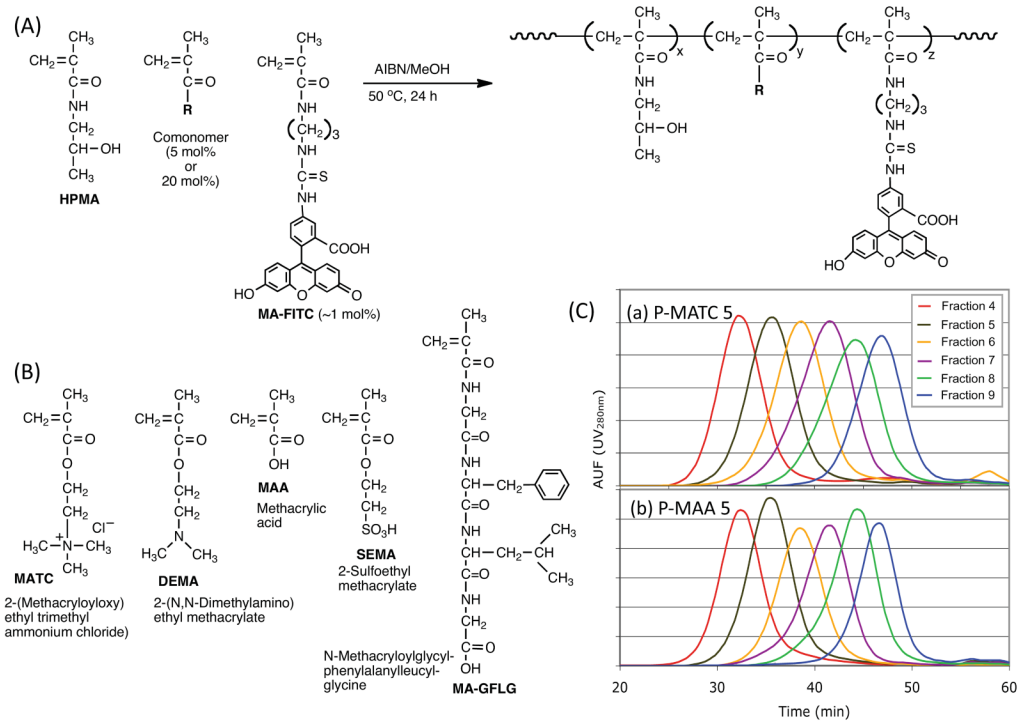

Scheme 1.

Synthesis of HPMA copolymers containing different functional groups. **A)** General synthetic scheme of the copolymerization of HPMA with functionalized comonomers. **B)** Structure of comonomers used to produce the copolymer array. **C)** Comparison of molecular weight distribution profiles of P-MATC5 (a) and P-MAA5 (b) fractions.

Table 1

Composition of HPMA copolymers containing different functional groups

Copolymer	Abbr.	Category	Content of comonomers (M)					
			M 1	Mol %	Wt %	M 2	Mol %	Wt %
P(HPMA-MAA 5%)	P-MAA5	Weak acid	MAA	4.8	2.89	FITC	0.67	2.49
P(HPMA-MAA 20%)	P-MAA20		MAA	18.2	11.6	FITC	0.65	2.56
P(HPMA-SEMA 5%)	P-SEMA5	Strong acid	SEMA	3.9	5.11	FITC	0.78	2.80
P(HPMA- SEMA 20%)	P-SEMA20		SEMA	18.0	22.5	FITC	0.74	2.53
P(HPMA-DEMA 5%)	P-DEMA5	Weak base	DEMA	4.7	5.06	FITC	0.59	2.15
P(HPMA- DEMA 20%)	P-DEMA20		DEMA	19.1	20.3	FITC	0.58	2.08
P(HPMA-MATC 5%)	P-MATC5	Strong base	MATC	4.4	6.17	FITC	0.55	1.97
P(HPMA-MATC 20%)	P-MATC20		MATC	16.5	22.0	FITC	0.58	1.96
P(HPMA)	P-FITC	Neutral	-	-	-	FITC	0.54	2.00
P(HPMA-GFLG 5%)	P-GFLG	Hydrophobic peptide	MA-GFLG	4.0	15.5	FITC	0.52	1.67

Table 2

Molecular weight, polydispersity and ζ Potential of HPMA copolymers containing charged groups

Copolymer	Category	Fraction 3		Fraction 6		Fraction 6
		Mw	Mw/Mn	Mw	Mw/Mn	ζ Potential
P-MAA5	Weak acid	203	1.15	60	1.1	−15.5±1.3
P-MAA20		158	1.15	78	1.2	−21.1±1.7
P-SEMA5	Strong acid	151	1.2	54	1.1	−16.8±1.5
P-SEMA20		176	1.15	58	1.2	−35.6±2.3
P-DEMA5	Weak base	150	1.15	50	1.15	10.6±0.7
P-DEMA20		156	1.06	61	1.16	17.6±0.9
P-MATC5	Strong base	194	1.13	52.1	1.15	12.7±1.1
P-MATC20		174	1.15	58.1	1.18	25.5±1.9
P-FITC	Neutral	142	1.07	59	1.09	3.36±1.4

Mw and Mn in kDa, ζ Potential, mV

Table 3

The summary of the extent of relative contribution of each pathway to endocytosis

Copolymers	CME	CaME	DDE	MPC
P-FITC	++	−	++	++
P-SEMA5	++	−	+	++
P-SEMA20	+	−	+	+
P-MAA5	++	−	++	++
P-MAA20	++	−	+	++
P-DEMA5	++	−	++	++
P-DEMA20	++	−	+++	+++
P-MATC5	++	−	++	++
P-MATC20	++	−	+++	++

The decrease of uptake compared to control in the range of 1–25% (+), 26–50% (++), 51–75% (+++) and 75–100% (++++) in response to inhibition. CME: Clathrin-mediated endocytosis, CaME: Caveolae-mediated endocytosis, DDE: Dynamin-dependent endocytosis, MPC: Macropinocytosis.